In Situ Syntheses of a Suspension Agent Based on a Styrene–Acrylic Acid Copolymer for the Suspension Polymerization of Styrene

Leopoldo Vilchis,[1] Leonardo Ríos,[2] Marco A. Villalobos,[3] Alain Guyot[4]

[1]*Departamento de Ingeniería Química, Facultad de Química, UNAM, Circuito Escolar, Ciudad Universitaria, 04510, México D. F.*
[2]*Centro de Investigación y Desarrollo Tecnológico, Girsa Corporativo SA de CV, Av. de los Sauces 87 Mz. 6, Parque Industrial Lerma, 52000, Lerma, Edo, México, México*
[3]*S. C. Johnson Polymers, 1525 Howe Street, Racine, Wisconsin 53403-2236*
[4]*Laboratoire de Chimie et Procédés de Polymérisation, LCPP/CNRS-CPE, 43, Bd. du 11 Novembre 1918, Bâtiment 308 F, B. P. 2077, 69100 Villeurbanne, France*

Received 2 November 2000; accepted 13 November 2001

ABSTRACT: We carried out the suspension polymerization of styrene, initiated with benzoyl peroxide at 80°C, in the presence of the simultaneous polymerization of acrylic acid in the water phase, initiated by potassium peroxidisulfate (KPS) at the same temperature. The polymerization in the water phase was started at certain times after the beginning of the polymerization of styrene. Then, a continuous addition of KPS was carried out at a given landing rate and during variable feeding times. The water-phase polymerization actually produced a copolymer of styrene and acrylic acid, which displayed surface-active properties. The particle size distribution depended on the variables mentioned earlier (starting time, KPS feeding rate, and addition time), being controlled by the molecular weight, and on the composition of the copolymer produced and its availability at the increasing conversion of styrene. A second distribution of submicronic particles was produced. Both families of particles had about the same molecular weight. © 2002 Wiley Periodicals, Inc. J Appl Polym Sci 86: 3271–3285, 2002

Key words: particle size distribution; stabilization; water-soluble polymers; surfactants

INTRODUCTION

In the suspension polymerization process, monomers rather insoluble in water and oil-soluble initiators are dispersed as liquid droplets by the action of vigorous stirring. The system is considered a turbulence-stabilized dispersion, which is unstable on cessation of agitation, coalescing and separating into two distinct phases. Figure 1 shows schematically the generally accepted the mechanism of formation of the suspension. Mechanical agitation subjects the bulk monomer phase to a viscous drag, causing elongation into a threadlike form with subsequent degeneration into drops. Simultaneously, through the reverse process of coalescence, the drops tend to revert to the original monomer mass. In a simple mechanical suspension under a constant overall shear rate, a dynamic equilibrium is quickly established. Clusters of globules, which are held together by weak residual forces but are not fused, tend to disperse under the disruptive stress of the stirrer. Efficient surface-active agents alone will deflocculate these aggregates. With the onset of polymerization and the corresponding increase in viscosity of the organic phase, there is increasing resistance to distortion of the droplets due to viscous drag, but unfortunately, there is a greater tendency toward coalescence through collisions with neighboring drops. The latter phenomenon is minimized by suspension stabilizers, which are selectively adsorbed at the interface between the two phases, forming a protective film of molecular proportions.[1]

The control of particle size distribution (PSD) is one of the most important issues in the suspension polymerization. Studies of drop sizes in liquid–liquid dispersion have demonstrated that the stirrer speed, interfacial tension, viscosities of both phases, and volume fraction of the dispersed phase has important effects on the droplet size.[2–4] In practice, some parameters, such as the geometry of the reactor or the stirrer and the operating parameters, are fixed by the productivity requirements and by polymerization kinetics. Consequently, the remaining parameters to establish a control of PSD are the stirring intensity and the type and concentration of stabilizer.

Correspondence to: A. Guyot.
Contract grant sponsor: CONACYT.
Contract grant sponsor: DGAPA-UNAM.
Contract grant sponsor: Ministère des Affaires Etrangers to PCP-2 México—France project.

Journal of Applied Polymer Science, Vol. 86, 3271–3285 (2002)
© 2002 Wiley Periodicals, Inc.

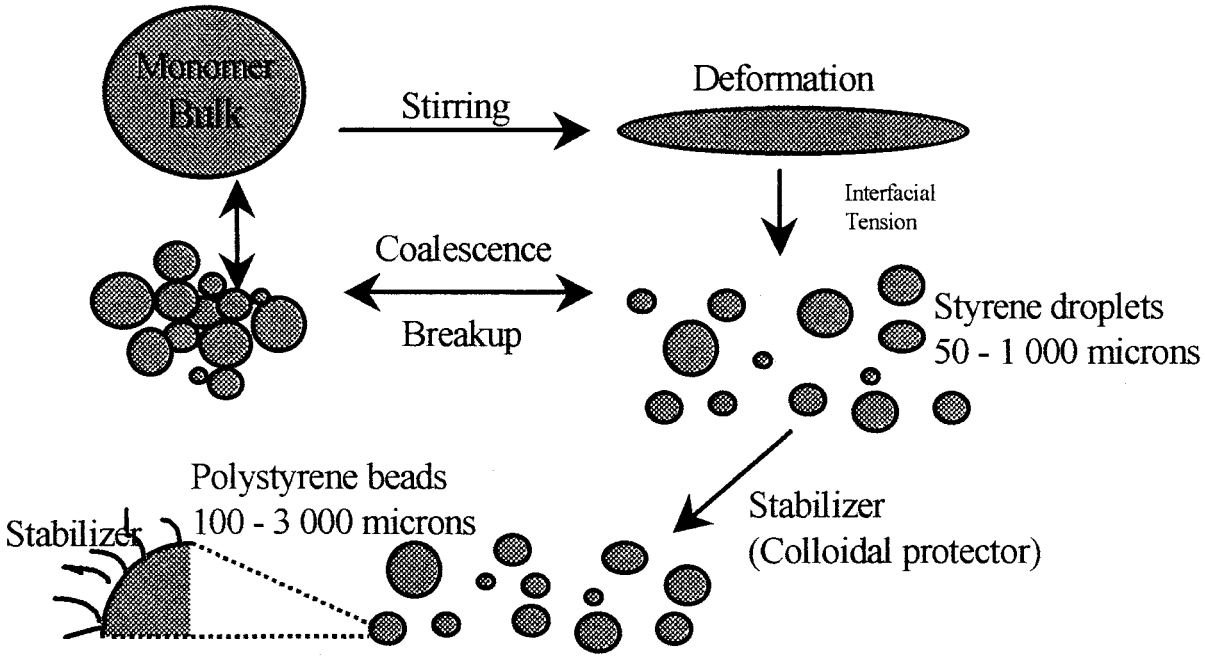

Figure 1 Schematic diagram of the states of dispersion in suspension polymerization.

The new idea explored in this work consisted of the *in situ* synthesis of a suspension agent. The formation of the suspension agent was achieved by the free-radical copolymerization of acrylic acid (AA) and styrene (STY) in the aqueous phase during the polymerization of STY in the dispersed phase, with potassium peroxidisulfate (KPS) as the initiator for the polymerization in the continuous phase and benzoyl peroxide (BPO) for the dispersed phase. The suspension agent formed by the *in situ* synthesis modified the interfacial tension between the monomer–polymer droplet and water, and it formed a film, or skin, around the monomer–polymer droplet surface to prevent coalescence by a mechanism similar to steric stabilization when collisions occurred. The variation of these two properties of the system as a function of the reaction time of the dispersed phase performed a control of the final PSD. The interfacial tension in this system depended on the suspension agent concentration, its composition, and its affinity to the interface. The formation of the protective film depended on the molecular weight of the suspension agent, its concentration, and its interfacial activity. Reports in the literature shows that a good polymeric stabilizer, although water soluble, should have enough hydrophobic character to be rather strongly adsorbed onto the surface of the particles and to stay at the interface of the two phases. Suspension polymerization uses low levels of protective colloid (~0.1 wt %) with little increase in the viscosity of the continuous phase. It has been admitted that the effect of interfacial adsorption is more important than the increase in viscosity of the aqueous phase when a suitable stabilizer is chosen.[4]

PSD in the suspension polymerization of sty

Normally, in a liquid–liquid dispersion in a turbulently agitated vessel, two regions are proposed to describe the breakup coalescence behavior of a droplet: the impeller region, where the droplets are broken up, and the circulation region, where they grow by coalescence. In the case of the suspension polymerization, the breakup and coalescence of the droplets maintain a balance during the reaction until the drops are transformed into solid particles due to the advancement of the reaction.[2,3] Turbulent fluctuation in the velocity over a distance at most equal to droplet diameter produces shear forces, which produce a deformation and finally a breakup of the droplet; however, the surface tension forces tend to hold the droplet together. Coalescence takes place when a collision of two droplets occur because the film of the continuous phase between the droplets is totally drained, so that the droplets touch and are fused in one; then, the droplet size always depends on the equilibrium of these rates (breakup and coalescence). The PSD evolution in suspension polymerization has been explained by correlations based on the Weber number theory.[4–6]

The suspension polymerization process can be divided into three stages with respect to the monomer conversion. In the first stage, when the viscosity of the dispersed phase remains low ($\eta < 1.0$ poise), the droplet size distribution results from the equilibrium between the breakup of the dispersed droplets due to the shear stress imposed by the stirring conditions. When the viscosity of the dispersed phase, due to the in-

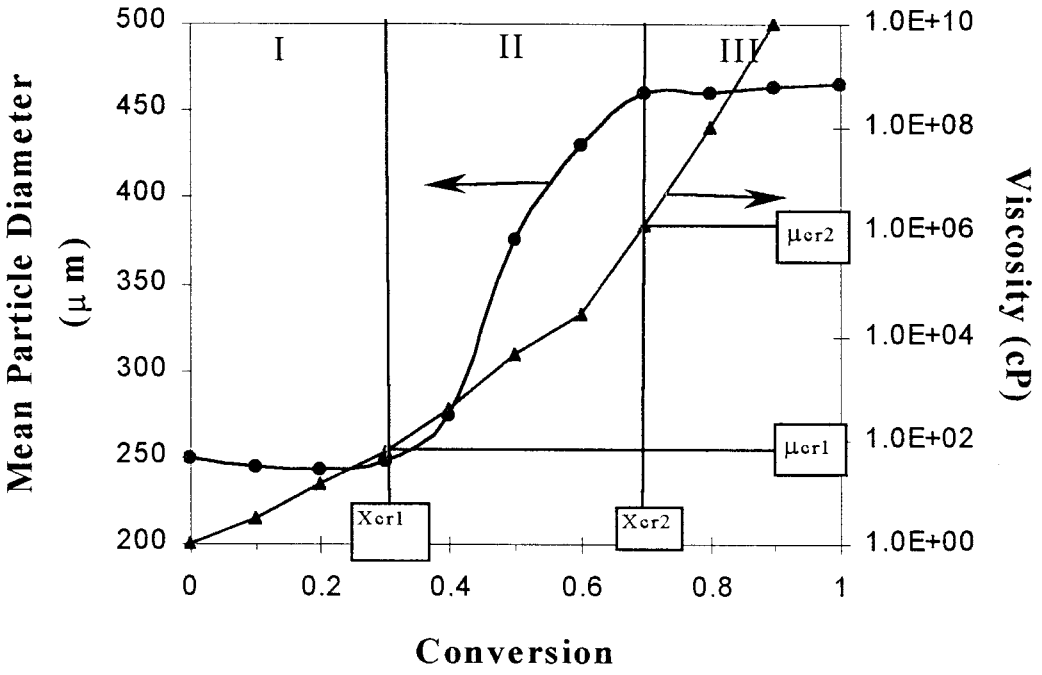

Figure 2 Dispersed phase viscosity and average particle diameter as a function of monomer conversion.

creasing conversion, reaches a critical value, ($\eta_{cr1} \approx 1$ poise), the coalescence tends to overcome the breakup, and the droplet size tends to increase (the *sticky point*); normally, the stabilizer tends to oppose the coalescence process, so that if it is present and efficient enough, the coalescence is delayed, and the particle size increases slowly. The end of the second stage, also named the *sticky stage,* takes place when the viscosity of the dispersed phase reaches a second critical value ($\eta_{cr2} \approx 10^3$ poise). The coalescence is avoided, the particle growth is stopped due to the elastic nature of the particle collisions, and the size of the particles remains fixed [the *particle identity point* (PIP)]. The corresponding conversion is the beginning of the third and last stage, where the PSD is fixed and consequently definitive.[7,8]

The stabilizer does not play any role in the third stage and is efficient only during the second sticky stage, when the viscosity of the dispersed phase is in between η_{cr1} and η_{cr2}. A typical evolution of the viscosity of the dispersed organic phase versus STY conversion is shown in Figure 2, where the evolution of the droplet diameter is also displayed, as well as the two critical viscosities.[9]

It can be seen that neither in the first stage nor in the third one does the droplet size change significantly. The stabilizers, which control the interfacial tension, are not useful in these two stages. They play a significant role only during the second stage, where they may control the growing process of the polymer particles.

Qualitatively, the *in situ* formation of the suspension agent in the continuous phase should begin at the end of the stage I or at the beginning of the stage II of polymerization of the dispersed phase (see Fig. 2). The *in situ* synthesis of stabilizer should be possible if the polymerization rate in the continuous phase is accurately synchronized with the rate of polymerization of the particles in the dispersed phase. The polymerization rate of the suspension agent in the continuous phase should be such that a large enough amount of the suspension agent has been produced at the point when the coalescence is maximum and the rupture of the polymerization is minimum. This point is experienced by the system practically at the end of the second interval.[10]

In situ polymerization model

The *in situ* synthesis of suspension agent is determined by the kinetics parameters of the system, initiator, and monomer concentrations and the partition between the liquid phases. The kinetic model for free-radical polymerization, adapted from a comprehensive model for addition polymerization, was the basis for our polymerization model.[11–13] The reactions affecting the aqueous-phase and dispersed-phase radical species of our process are listed in Table I.

In the case of polymerization in the water phase, the effect of the monomer concentration in the formation of primary radicals is included in the reaction mechanism. This behavior of the AA polymerization has been reported in several publications, and it has been explained by participation of the monomer in the dissociation of the peroxidisulfate ions (I^w_{KPS}). The AA (M^w_1) molecules assist the formation of the primary

TABLE I
Reactions Affecting Aqueous and Dispersed Phase Polymerization

	Continuous Phase	Dispersed Phase
Initiation	$I^w_{PS} \xrightarrow{k_d} (2R_C)^w$	$I^D_{BPO} \xrightarrow{KD} 2R^D_1$
	$(2R_C)^w + M^w_1 \xrightarrow{k'} R^w_{1,1} + R^w_1$	$R^D_1 + M^D_j \xrightarrow{KI} R^D_{1,j}$
	$R^w_1 + M^w_j \xrightarrow{k''_j} R^w_{1,f}$	
Propagation	$R^w_{n,i} + M^w_j \xrightarrow{kp_{ij}} R^w_{n+1,j}$	$R^D_{n,i} + M^D_j \xrightarrow{kp_{ij}} R^D_{n+1,j}$
Termination	$R^w_{n,i} + R^w_{m,j} \xrightarrow{ktc_{ij}} P^w_{n+m}$	$R^D_{n,i} + R^D_{m,j} \xrightarrow{ktc_{ij}} P^D_{n+m}$
Transfer to monomer	$R^w_{n,i} + M^w_j \xrightarrow{ktrm_{ij}} P^w_n + R^w_{1,j}$	$R^D_{n,i} + M^D_j \xrightarrow{ktrm_{ij}} P^D_n + R^D_{1,j}$
Capture of radicals by droplets	$R^w_{n,i} + G \xrightarrow{kcap_i} R^D_n$	
Desorption of radicals from droplets	$R^D_{n,i} \xrightarrow{kdes_i} R^w_{n,2}$	

G = droplet.

radical trapped in a "cage structure" $(2R_C)^w$.[14,15] This effect results in a 3/2 dependence of the polymerization rate with respect to monomer concentration. M^w_j refers to monomers (j = 1 for AA and 2 for STY), $R^w_{n,i}$ and P^w_n refer to live polymer radicals and dead polymer, respectively, of length n with monomer type i at the growing end, in the water (w) or continuous phase. In the case of dispersed phase polymerization $R^D_{n,i}$ refers to live polymer radicals of length n with monomer type i at the growing end, and D refers to the dispersed phase. To simulate both simultaneous polymerizations, the following assumptions were incorporated into the model: (1) the stationary-state hypothesis and long-chain hypothesis were assumed valid for all radical species, and (2) the quasistationary of the instantaneous copolymer composition was assumed. When these assumptions are valid, it is possible to model the kinetics of both phases, dispersed and continuous phase. A total balance for the AA and STY gives

$$\frac{dM_1}{dt} = -V^w(kp_{11}[R^w_1][M^w_1] + kp_{21}[R^w_2][M^w_1] + ktm_{11}[R^w_1][M^w_1] + ktm_{21}[R^w_2][M^w_1]) - V^D(kp_{11}[R^D_1][M^D_1] + kp_{21}[R^D_2][M^D_1] + ktm_{11}[R^D_1][M^D_1] + ktm_{21}[R^D_2][M^D_1]) \quad (1)$$

$$\frac{dM_2}{dt} = -V^D(kp_{12}[R^D_1][M^D_2] + kp_{22}[R^D_2][M^D_2] + ktm_{12}[R^D_1][M^D_2] + ktm_{22}[R^D_2][M^D_2]) - V^w(kp_{12}[R^w_1][M^w_2] + kp_{22}[R^w_2][M^w_2] + ktm_{12}[R^w_1][M^w_2] + ktm_{22}[R^w_2][M^w_2]) \quad (2)$$

where $[M^f_j] = M_j/V^f$ is the monomer j concentration at time t in the reactor, V^f the volume of f phase, and $[R^f_j]$ is the total live polymer concentration with monomer type j at the growing end:

$$[R^f_j] = \sum_{n=1}^{\infty} [R^f_{n,j}] \quad (3)$$

The STY and AA consumptions take into account the reactions in water and in the droplets, and we modeled the partition of monomers in the different phases considering that a fast thermodynamic equilibrium is achieved. The partition coefficients (K'_j) of each monomer is defined as follows:[16,17]

$$K'_j = \frac{[M^D_j]}{[M^w_j]} \quad (4)$$

The last two terms of the kinetics mechanism were excluded in the model because the interfacial area was

not very important due to the fact that the mean droplet diameter was large (~100 μm). Then, capture and desorption of water radicals by the droplet were negligible in the suspension polymerization. Moreover, the addition of an oil-soluble initiator such as BPO and a water-soluble initiator such as KPS could hinder both phenomena. A detailed description of this approach is given in the Appendix.

Viscosity to zero shear of the polymerizing reaction mixture in the dispersed phase was estimated as a function with a correlation found in the literature, relating the polymer fraction in the dispersed phase, its molecular-weight average, and the temperature of the system:[18]

$$\log_{10}(\eta_0) = -12.116 + 1496T^{-1} + M_w^{0.2845} \times [8.679x_p - 15.024x_p^2 + (2.828 + 4500T^{-1})x_p^3] \quad (5)$$

where η_0 is the zero shear viscosity (poise), T is the temperature in Kelvin, x_p is the weight fraction of the polymer, and M_w is the weight-average molecular weight in thousands.

Interfacial activity of the suspension agents

Few selection methods of the stabilizer for suspension polymerization are reported in the literature due to the high complexity of the phenomenon of adsorption of soluble polymers at liquid–liquid and liquid–solid interfaces in suspension polymerization. Mendizabal et al.[19] proposed a method for selecting a poly(vinyl alcohol) (PVA) for STY suspension polymerization without carrying out polymerization reaction: the stability of the nonreacting systems is issued to predict the stability of the same system when it is reacting. Olayo et al.[20] studied the effect of the degree of hydrolysis and of the molecular weight of PVA on the interfacial tension of the STY/water–PVA systems and, by the Szyszkowski model, related the interfacial activity of the PVA to the stability of the STY suspension polymerizations.

The Szyszkowski model correlates the interfacial tension with the bulk concentration of the stabilizer at a constant temperature:

$$\Pi = \gamma - \gamma_0 = -\Gamma_s^* K^* T^* \mathrm{In}(1 + \beta C) \quad (6)$$

where Π is the difference of the interfacial tension of the pure phases (γ_0) and the interfacial tension of stabilizer solutions (γ, dyne/cm), Γ_s is the interfacial stabilizer concentration when the interface is saturated (molecules/cm^2), K is the Boltzman constant, T the temperature in Kelvin, β is the adsorption intensity, and C is the bulk concentration of the stabilizer. The Gibbs equation proposes a relationship between the amount of adsorbed stabilizer and the change of interfacial tension in function of the stabilizer concentration:

$$\Gamma_2 = -\left(\frac{C}{KT}\frac{d\gamma}{dC}\right)_T = -\left(\frac{1}{KT}\frac{d\gamma}{d\ln C}\right)_T \quad (7)$$

The substitution of eq. (6) in eq. (7) gives

$$\theta = \frac{\Gamma_2}{\Gamma_S} = \frac{Cd\ \ln(1 + \beta C)}{dC} = \frac{\beta C}{1 + \beta C} \quad (8)$$

where Γ_2 is the interfacial concentration of the stabilizer (molecules/cm^2) and θ is the surface coverage. Equation corresponds to the Langmuir isotherm equation.

It is clear that the adsorption of soluble polymers at liquid–liquid and solid–liquid interfaces is a highly complex phenomenon. The polymer chains could have a large number of possible configurations at the interface. The Langmuir isotherm assumes that there is a single average configuration of the molecule at the interface. However, macroscopic models for polymers adsorption, which take into account the number of segments of molecules attached at the interface and individual adsorption constants for every segment, are reduced to the Langmuir form at high surface coverage.[21]

EXPERIMENTAL

The experiment was divided in two parts. In the first part, the partition of the monomers under our reaction conditions was studied, and in the second part, the *in situ* syntheses of stabilizers were performed.

Materials

AA (Aldrich, Milwaukee, WI) was purified by vacuum distillation. KPS, BPO, STY, tetrahydrofuran (THF), and toluene (Aldrich) were used without any purification, and deionized water was used in the reaction system.

Partitioning of AA and STY

A mixture of water, STY, and AA was placed in a hermetically closed vial and mixed vigorously with a shaker for 30 min to attain partition equilibrium. The vial was placed in a water bath at 80°C. Table II shows the recipes used in the experiments. After the phase separation, samples of 1.0 g were drawn from each phase and dissolved in 12 mL of THF previously prepared with toluene as an internal standard. The concentrations of STY and AA were measured, respectively, in each phase by gas chromatography (5890

TABLE II
Determination of the Monomers Partition at 80°C

Water (g)	AA (g)	STY (g)	Weight fractions in the aqueous phase		Weight fractions in the dispersed phase	
			X_{AA}	X_{STY}	X_{AA}	X_{STY}
7.107	0.000	2.895	0.00	6.53×10^{-4}	0.00	1.000
7.081	0.031	2.883	0.389×10^{-2}	6.49×10^{-4}	1.05×10^{-4}	0.999
7.046	0.098	2.867	1.122×10^{-2}	6.46×10^{-4}	4.73×10^{-4}	0.999
7.001	0.150	2.854	1.997×10^{-2}	6.38×10^{-4}	10.38×10^{-4}	0.998

Hewlett Packard chromatograph with an HP-5 column of 0.25 μm and 25 m) (Avondale, PA).

Polymerization procedure

The suspension polymerization reactions of STY were carried out with two different concentrations of AA in a 2-L glass round-bottom reactor (see Fig. 3).[22] The operating conditions and the geometrical array of the reactor are described in Table III. The initiators selected for *in situ* synthesis were soluble in only one phase; KPS was the selected initiator for the continuous phase, and BPO was the initiator for the dispersed phase. The reaction water was preheated to 90°C in the reactor and stirred at 350 rpm; then, the STY with dissolved BPO was added into the reactor. After a few minutes (~3 min), the temperature was controlled at 80°C; the time when all STY mix was added to the reactor was named time zero of the reaction ($t = 0$). Starting time (ST) of the *in situ* synthesis of the suspension agent was defined by the ST of the semicontinuous addition of KPS solution, and it varied from 30 to 60 to 120 min after $t = 0$ (the beginning of dispersed-phase polymerization). The batch addition of AA was done 3 min before the ST. The feeding rate (FR) of the addition of KPS and the feeding time (FT), during which the semicontinuous addition of initiator was performed, were other variables in this work. Table IV shows the conditions of *in situ* syntheses. The reactions were stopped after 5 h, when the system reached and passed the PIP.

Individual conversions of STY and AA were followed during some experiments. A sample drawn from the reactor was dissolved in THF; the monomer concentrations was determined by the same technique (gas chromatography) used for the partition experiments, and water contained in the sample was determined by Karl–Fisher titration.

To compare this new process against the traditional suspension polymerization, we carried out four complementary experiments were carried out, three experiments with a commercial PVA (88% of hydrolysis and $M_w \approx 100{,}000$) and one experiment with a poly(acrylic acid) (PAA) synthesized in water solution with a M_w of approximately 80,000. A solution of PVA or PAA was prepared containing 14.25 g dissolved in 100 mL of water; the solution was added to the STY suspension polymerization at the same ST of the *in situ* reactions. The suspension polymerizations were carried out under the same conditions of temperature, BPO concentration, and agitation used in the *in situ* experiments (see Table V).

The polymer beads were separated by filtration on a 200 mesh filter and the final PSD was obtained by sieving, according to the ASTM D 1921 method. The serum was generally milky and contained an emulsion of small particles. These particles were separated on ultracentrifugation, leaving a clear solution of water-soluble copolymer. All the three kind of polymers were analyzed by size exclusion chromatography (Waters instrument, Model 510) to obtain their molecular-weight distribution. The compositions of reaction products were determined by ^{1}H-NMR, and molecular-weight distributions were determined by aqueous size exclusion chromatography (Waters, with polystyrene gel columns, calibrated with polyoxyethylene standards).

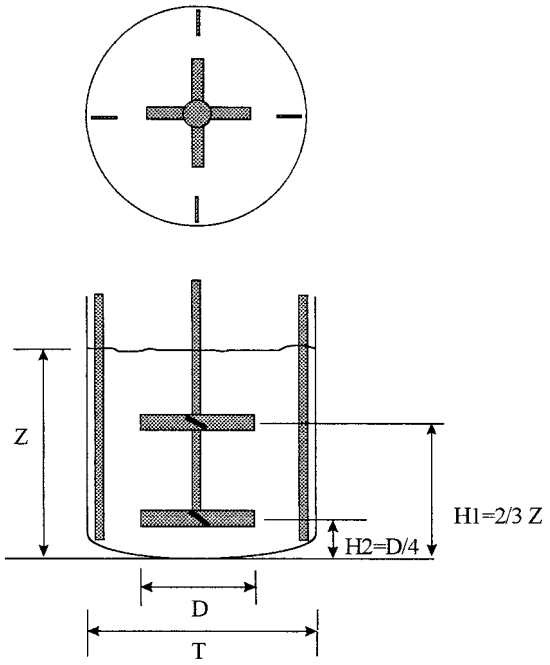

Figure 3 Schema of the internal array of the reactor.

TABLE III
Operating Conditions for Suspension Reactions and Geometrical Array of the Suspension Reactor

Parameter	Value
Initial volume at 25°C	V_0 = 1.500 L (1.0 L of water + 0.5 L of STY)
Dispersed/continuous volume phase at 25°C	Φ = 0.50
Initiator concentration (BPO)	$[BPO]_0$ = 0.037 mol/L of STY
Polymerization temperature	T = 353.15 K (80°C)
Polymerization time	t = 5 h
Agitation speed	N = 350 rpm
Internal diameter of vessel	T = 10.0 cm
Impeller diameter	D = 5.0 cm
Number of impellers	2
Impeller type	4-blade, 45° pitch
Blade width	W = 0.32 cm
Liquid height	Z = 20.0 cm
Position of bottom impeller	$H1$ = 5.0 cm = $T/4$
Position of top impeller	$H2$ = 13.3 cm = $(2/3)Z$
Number of baffles	Four every 90°

Finally, the interfacial tension of water-soluble product solution against STY was measured at 25°C by a Du Nouy ring method in a Kruss 12 tensiometer (Krüss GmbH, Hamburg, Germany).

RESULTS AND DISCUSSION

Partition of monomers

Figure 4 shows the experimental results for the equilibrium partitioning of AA between aqueous and organic phases at a natural pH of 2.6 and at 80°C. It was there clear that under these conditions, around 4 mol % of AA was present in the organic phase and 96% was in the water phase. As a consequence, the polymerization of AA took place mainly in the water phase because the presence of AA in the droplets was negligibly small, where its consumption should have been negligibly small compared to that of STY.

Figure 5 shows that the concentration of STY in the water phase remained practically constant at a concentration of about 0.045 mol/L. We can expect that the consumption of STY preferentially took place in the droplets, with a very small consumption in the continuous phase. However, its concentration in the water phase should have been enough to produce significant amounts of copolymers able to present some surface activity.

Polymerization in the dispersed and continuous phases

Clear particles with spherical shape with diameters on the order of a millimeter were obtained in all suspension polymerizations performed at a high initial AA concentration. The suspension particles were separated by a mesh 200 from the aqueous phase; the residual aqueous phase had whiteness coloration, and the presence of submicronic particles was observed. After an exhaustive centrifugation of the aqueous phase, the submicronic particles were separated, and the water-soluble product was recovered from the serum. The results of product characterization are

TABLE IV
Recipes of the *In Situ* Syntheses and Product Characterization

		Addition conditions of PPS			Water soluble polymer		Suspension particles		PSD analyses	
Experiment	AA (g)	ST (min)	FR (mg/min)	FT (min)	$M_w \times 10^{-4}$	STY (mol %)	Submicronic $M_w \times 10^{-3}$	Beads $M_w \times 10^{-3}$	D_m (mm)	STD (mm)
1	22.6	30	48.7	30	16.1	13.9	90	82	0.11	0.07
2	22.6	60	48.7	30	—	—	81	82	0.20	0.20
3	22.6	120	48.7	30	9.6	14.1	94	77	0.37	0.23
4	22.6	120	24.3	60	14.9	14.3	90	78	0.55	0.24
5	22.6	120	12.2	120	15.5	13.8	86	79	0.64	0.27
6	13.6	120	29.2	30	18.3	17.6	89	82	0.85	0.28
7	13.6	120	14.6	60	—	—	—	—	—	—
8	13.6	120	7.3	120	—	—	—	—	—	—

M_w = M_w in daltons; D_m = mean particle diameter; STD = standard deviation of PSD. The variables are ST (the time at which the AA polymerization was started), FR of KPS addition, and FT, during which the addition of KPS was performed.

TABLE V
Recipes of the Traditional Suspension Polymerization with PVA and PAA

	Stabilizer (g)	Addition time (min)	Submicronic $M_w \times 10^{-3}$	Beads $M_w \times 10^{-3}$	PSD analyses D_m (mm)	PSD analyses STD (mm)
	PVA					
9	14.25	30	90	81	0.44	0.82
10	14.25	60	86	79	0.34	0.43
11	14.25	120	Coalescence		—	
	PAA					
12	14.25	30	Coalescence		—	
13	14.25	0	Coalescence		—	

D_m = mean particle diameter; STD = standard deviation of PSD.

summarized in Table IV. The average molecular weights of the polystyrene beads and submicronic particles had about the same values, and the reaction time to reach the PIP was always around 4.5 h for all experiments. These data indicate that there was no influence of the suspension agent on the polymerization kinetics of the dispersed phase polymerization.

Figure 6 shows the ^{1}H-NMR spectra of water-soluble product with the typical peaks of CHα and CH$_2\beta$ of the PAA backbone between 0.7 and 3.2 ppm, aromatics protons of the STY units in the copolymer between 6.5 and 8.5 ppm, and finally, a sharp peak between 9.0 and 12.0 ppm for the carboxyl proton. The integration of CHα, CH$_2\beta$, and aromatic peaks gave the global compositions a water-soluble product. As pointed out previously, it was evident that a copolymerization occurred in the continuous phase.

The analyses of ^{1}H-NMR of both sizes of particles obtained in the *in situ* experiments showed that the AA was not detected in the composition of the polymeric chain. Only the peaks of CHα and CH$_2\beta$ of the backbone between 1.2 and 2.5 ppm and of aromatics protons between 6.2 and 7.3 ppm were observed in the spectra (see Figs. 7 and 8). A copolymerization could have occurred in the dispersed phase only after the moment of the addition of the AA to the reaction system; however, due to very low fraction of AA in the dispersed phase, the polymer had very few molecules of AA in the backbone, not even detectable for the ^{1}H-NMR analyses.

Figure 9 shows the simulation results and the experimental data of the STY conversion and the estimate of the viscosity with eq. (5) for experiments 1, 4, and 5. The high polymerization rate of our experimental conditions produced a rapid increase of the dispersed phase viscosity after 60 min of reaction. We assumed that after this reaction time, the η_{cr1} was reached, and this marked the beginning of the second stage of the reaction. Konno et al. reported the same zoning values of the viscosity to mark the separation between the first and second stages. After 200 min of reaction, the viscosity was very high (conversion $\approx$ 0.70), so we considered that the growth or sticky stage of droplets was between these two reaction times.

Figure 10 shows the estimated values of the mean molecular weight and average molecular weight plotted as a function of the reaction time and against the experimental determination. In these two last figures,

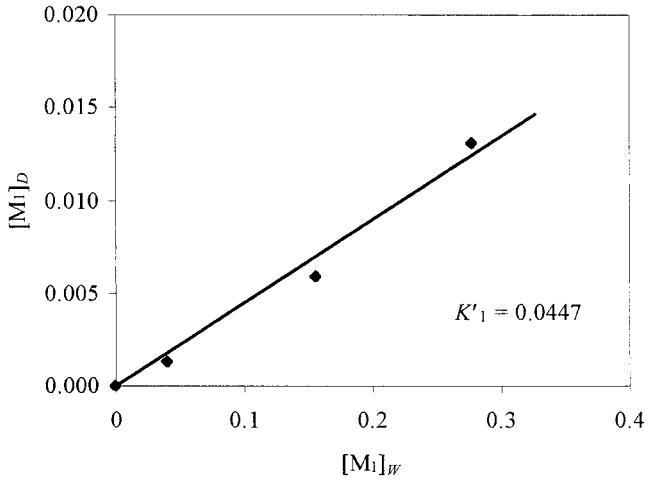

Figure 4 Partition coefficient of AA at 80°C and at a volume phase ratio $\phi = 0.5$.

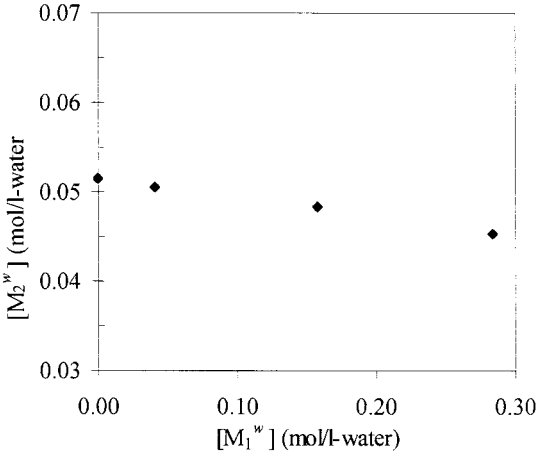

Figure 5 STY concentration ($[M_2]_W$ in mol/L of water) as function of AA concentration ($[M_1]_W$ in mol/L of water) in the water phase.

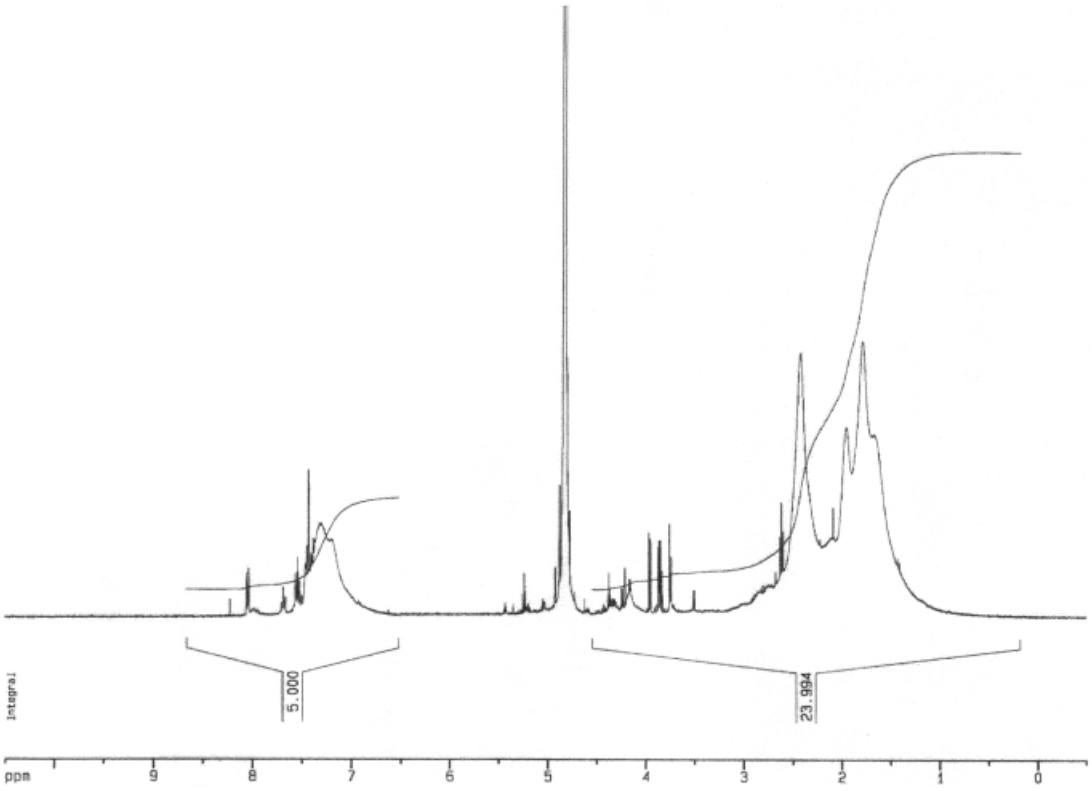

Figure 6 ^{1}H-NMR spectrum of the water-soluble polymer in experiment 1.

we observed that the simulation of the kinetics of the STY polymerization in the dispersed phase had good agreement with experimental data; a slight autoacceleration phenomenon was found at around 70% of monomer conversion (the parameters used in the simulation are in Table VI).

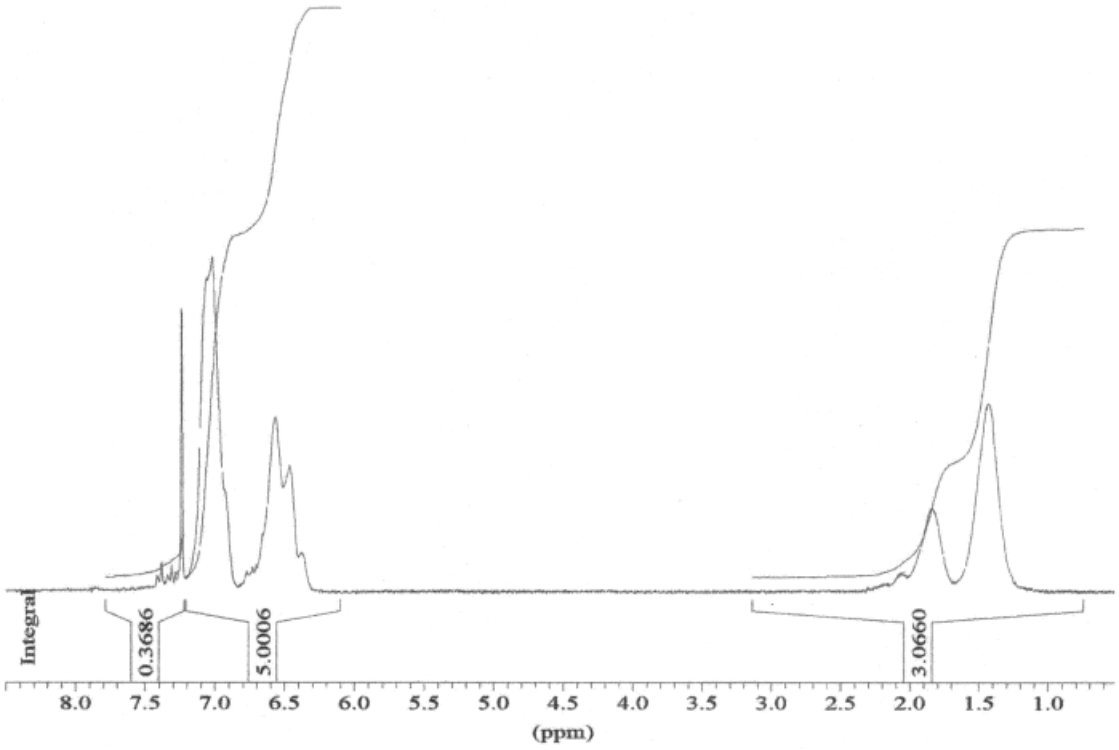

Figure 7 ^{1}H-NMR spectrum of the polymer formed in the droplets in experiment 1.

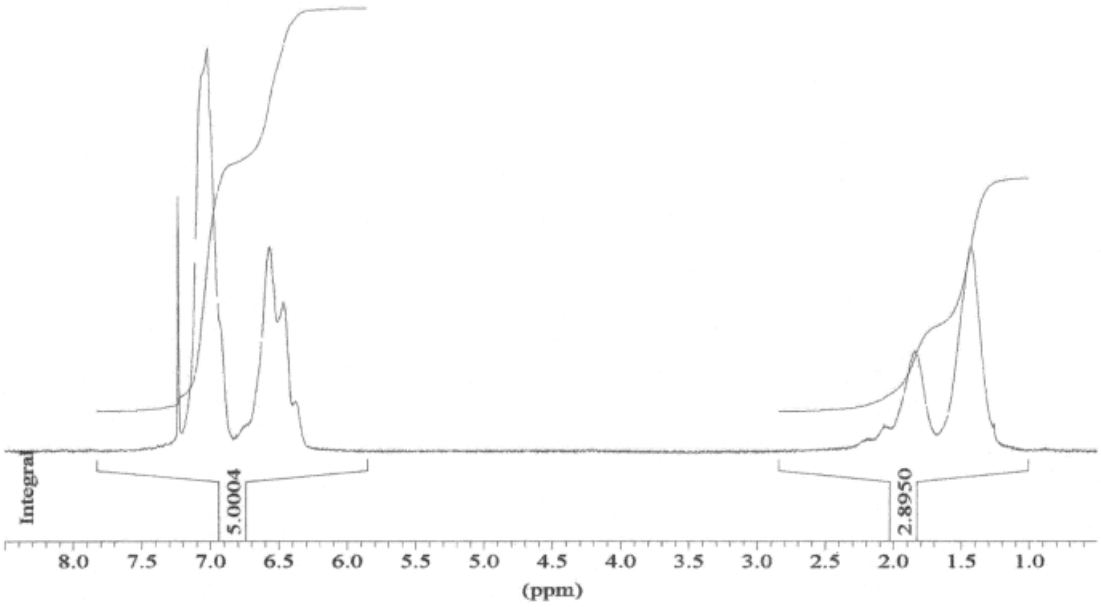

Figure 8 ^{1}H-NMR spectrum of the polymer formed in the submicronic particles in experiment 1.

Figures 11 and 12 show experimental data of the AA conversion followed in experiments 1, 4, and 5 and in the simulation results. The AA conversion reached high values in the first moments of KPS addition, but when the KPS addition was stopped, the rate of polymerization decreased considerably, and finally, the conversion was stopped, probably due to the total KPS dissociation, as can be seen from the dotted lines of Figure 11.

Final PSDs

In our reaction system, we detected that the η_{cr1} and the η_{cr2} were about 50 and 3000 cP, respectively. The corresponding conversions X_{cr1} and X_{cr2} were about 0.30 and 0.70, respectively, and reaction times of the dispersed phase for these critical values were around 60 and 200 min.

The effect of the ST (of the *in situ* synthesis of suspension agent) on the final PSD was studied first. Three different STs from the beginning of dispersed phase polymerization were used to start the water-phase polymerization. Figure 13 shows the final PSDs of these first three experiments. In experiment 1 (ST = 30 min), the system was in the early stage, and the viscosity was below 20 cP; the high production rate of the suspension agent provided a good stabilization of the dispersed phase and prevented the coalescence during the whole reaction. Then, the drop size re-

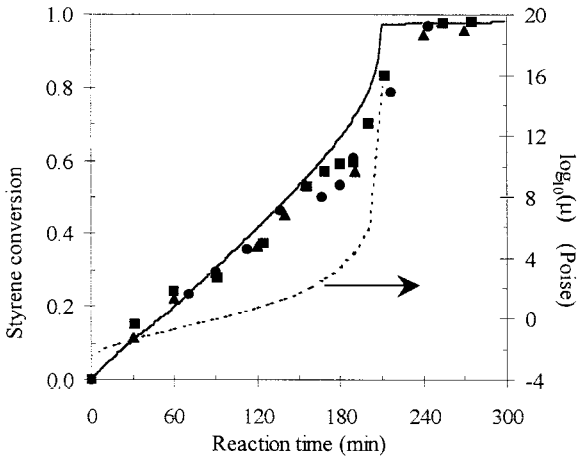

Figure 9 STY conversion and estimated dispersed-phase viscosity versus reaction time. Experimental points: (■) experiment 1; (★) experiment 4, and (▲) experiment 5. Predictions of the model for the (—) conversion and (– – –) viscosity.

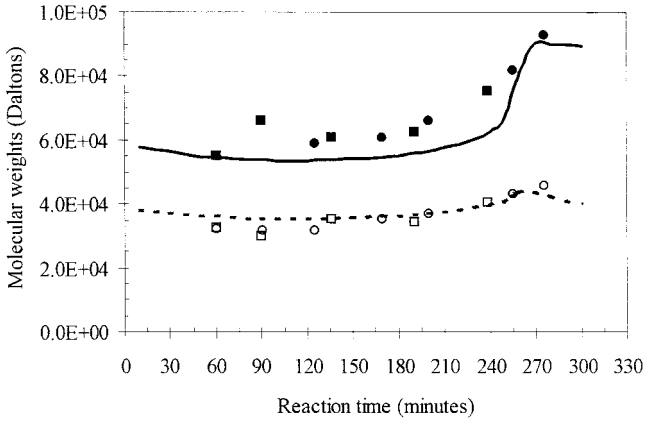

Figure 10 Molecular weights of polystyrene as a function of reaction time. (– – –) Model predictions for number-average molecular weight (M_n) and (—) model predictions for M_w. (□) Experimental M_n of experiment 1, (■) experimental M_w of experiment 1, (○) experimental M_n of experiment 4, and (●) experimental M_w of experiment 4.

TABLE VI
Parameters and Values Used in the Kinetic Polymerization of STY

Parameter and value	Units	Reference
$kp_{11} = 3.60 \times 10^9 \exp(-3100/RT)$	L/mol min	15
$ktc_{11} = 1.08 \times 10^9$	L/mol min	15
$r_1 = 0.13$		13
$KD_{BPO} = 4.16 \times 10^{15} \exp(-29{,}270/RT)$	L/min	12
$kp_{22} = 6.306 \times 10^8 \exp(-7068/RT)$	L/mol min	12
$ktm_{22} = 6.128 \times 10^{10} \times \exp(13{,}450/RT)$	L/mol min	12
$ktc_{22} = 7.550 \times 10^{10} \times \exp(-1677/RT)$	L/mol min	12
$r_2 = 0.38$		13
$R = 1.987$ cal/mol K		

Transfer to monomer and gel effect parameters are described in ref. [12].

mained unchanged around 100 μ. When the ST was changed and took place at the beginning of the second stage (ST = 60 min), the particles had began to grow, and the dispersed phase viscosity was about 60 cP; with large particles appearing as a tail of the PSD; however, 50% of the mass remained with small size. At ST = 120 min, the dispersed phase viscosity was about 800 cP, and the coalescence dominated over the breakup. The high production rate of the suspension agent could have prevented the full coalescence of the system and stabilized the particles with large sizes. This shift of the PSD could be assigned to growth of particles, due to the increment of viscosity of the dispersed phase when the formation of the suspension agent was started.

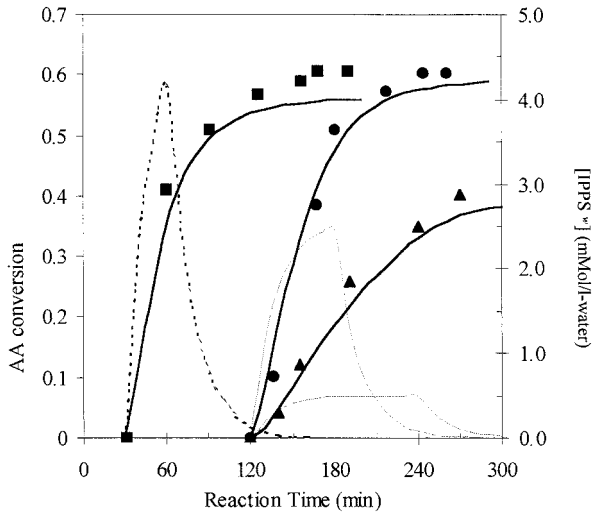

Figure 11 AA conversion as a function of reaction time during the *in situ* formation of the suspension agent. Experimental points: (■) experiment 1, (●) experiment 4, and (▲) experiment 5. (—) Predictions of the model for AA conversion and (– – –) estimation for initiator concentration.

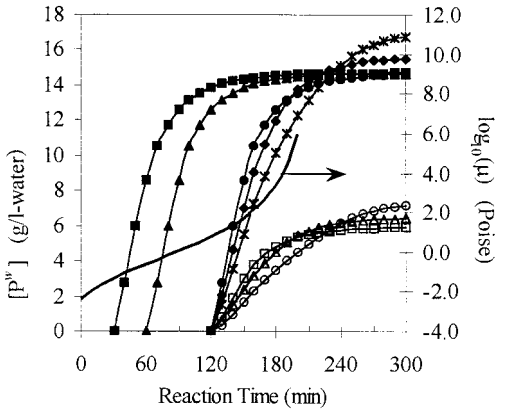

Figure 12 Predictions of the model for the water soluble polymer concentrations [P^w]: (■) experiment 1, (▲) experiment 2, (●) experiment 3, (◆) experiment 4, (*) experiment 5, (□) experiment 6, (△) experiment 7, and (○) experiment 8.

The effect of the polymerization rate of the suspension agent was studied as a second variable. Changes on the FR (of KPS) modified the polymerization rate in the water phase. Figure 14 presents the final PSD for experiments 3–5. In the middle stage, the particle size showed a high dependence on the stabilizer concentration; the maximum coalescence was around 190–210 min, and the dispersed phase viscosity changed from 100 to 2500–3500 cP during this period. At each time, the system had to reach equilibrium as a function of stabilizer concentration, interfacial area, and coalescence rate. When the initiator FR decreased, a growth on the particle sizes was observed. When the initiator FR was reduced, the polymerization rate was affected, and consequently, the stabilizer concentration was reduced during the critical coalescence period of the system (120–150 min); small differences in the stabilizer concentration in each experiment (3–5) showed an important influence on the particle sizes.

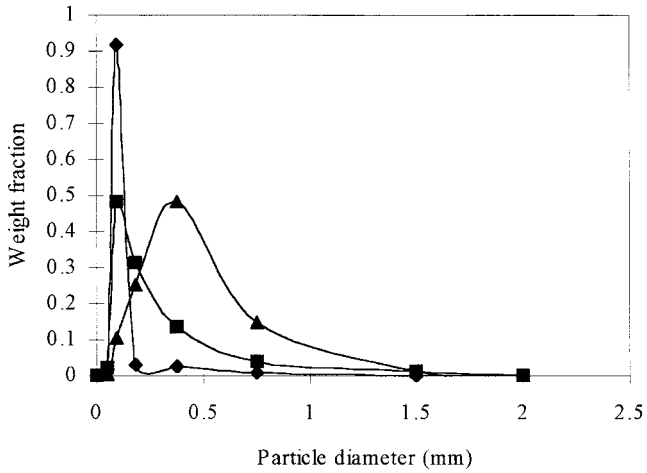

Figure 13 Effect of ST on the final PSD of polystyrene. ST = (◆) 30, (■) 60, and (▲) 120 min.

At 140 min of reaction, the amounts of stabilizer produced were 8.5, 7.1, and 5.8 for experiments 3, 4, and 5, respectively. The low stabilizer concentrations of experiments 4 and 5 in this period could not efficiently prevent the coalescence, and a shift of the PSD to large sizes occurred and caused a reduction of the interfacial area until the equilibrium on the system was reached.

In the third series of experiments, a reduction of the AA concentration was tried with a ST of 120 min and FTs of 30, 60, and 120 min. Here again, the ST was at the end of middle interval, where the stabilizer concentration had an important effect on the stability of the system. Only the stabilizer concentration of experiment 6 prevented the full coalescence of the system. In experiments 7 and 8, the stabilizer concentration during the critical period of coalescence was not high enough, and stable dispersions could not be maintained. Figure 15 shows the effect of AA concentration on the final PSD (experiment 3 [AA] = 23.8 g/L of water and experiment 6 [AA] = 14.3 g/L of water).

In the case of the traditional suspension polymerization carried out with PVA, the system was stable only when the addition of the solution was at 30 and 60 min after the ST of the dispersed-phase polymerization. When the addition was at 120 min after the ST, the suspension collapsed at around 200 min of reaction. This effect could be attributed to a maximum coalescence at that point; the effective stabilizing layer had not yet formed, and the coalescence frequency was not quickly controlled. Then, the system became unstable, and the stability of the suspension was lost during this stage. In the case of the suspension reaction with PAA as a stabilizer, any reaction was stable, even if the addition of solution was at the beginning of the polymerization of the dispersed phase. The high hydrophilic character of the homopolymer molecules did not allow a strong enough adsorption at the droplet–water interface. If

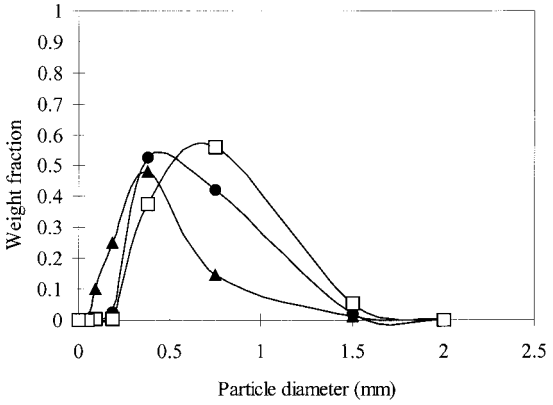

Figure 14 Effect of the FR of KPS on the final PSD of polystyrene at a high AA concentration ([M_1] = 25.1 g/L of water). FR = (▲) 48.7, (■) 24.3, and (□) 12.2 mg/min.

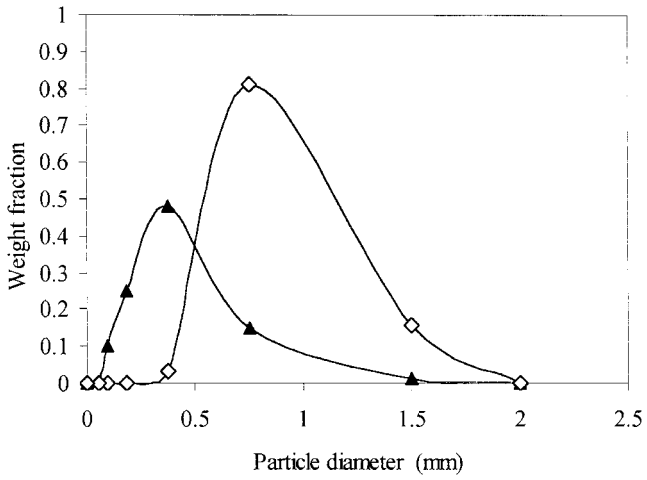

Figure 15 Effect of AA concentration on the final PSD of polystyrene: (▲) experiment 3 and (♦) experiment 6.

the polymer is not strongly adsorbed, desorption may occur during a particle collision. The total coalescence of droplets could not be prevented before the system reached the PIP.

Figure 16 shows the final PSD of experiments 1, 2, 9, and 10. The suspension agents formed by the *in situ* process had better performance avoiding the coalescence than PVA in the traditional process. In experiments 1 and 2, the intensity of the growth was better limited by the efficiency of the stabilizing layer of the *in situ* agent, and their final PSDs remained in the small sizes. In experiments 9 and 10, the growth of the particles should have happened until the breakage–coalescence equilibrium was established by the efficiency of the protective layer.

It is well known that the thickness of the adsorbed polymer increases with the molecular weight, and then, the coalescence is better prevented by higher molecular weights.[23]

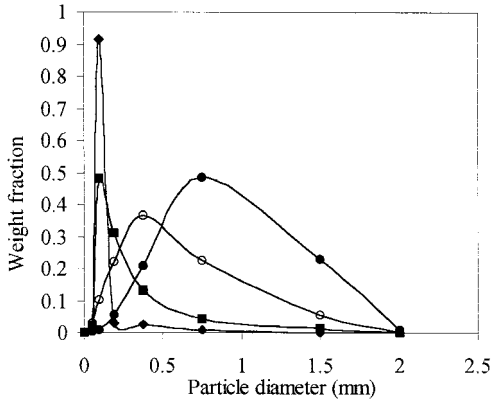

Figure 16 Effect of the process and kind of suspension agent on the PSD. *In situ* process: (◆) experiment 1 and (■) experiment 2. Traditional process with PVA: (●) experiment 9 and (○) experiment 10.

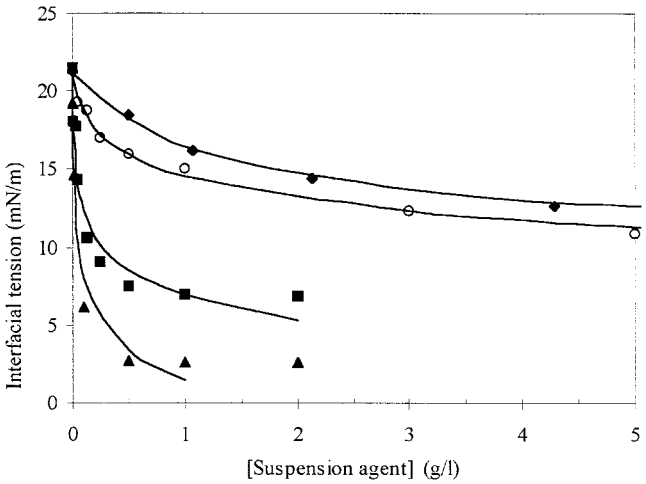

Figure 17 Interfacial tension of several suspension agents: (▲) experiment 6, (■) experiment 1, (○) PVA, and (◆) PAA.

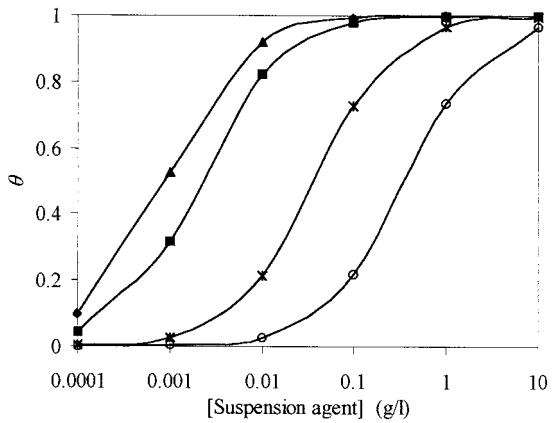

Figure 18 Adsorption isotherms for the suspensions agents: (▲) experiment 6, (■) experiment 1, (○) PVA, and (◆) PAA.

Properties of the suspension agents at the interface

The *in situ* synthesized water-soluble copolymers showed a strong influence on the interfacial tension. Figure 17 shows the behavior of the interfacial tension of several water solutions of suspension agents against STY as a function of their concentrations. A large decrease in interfacial tension was observed at very low concentrations of the *in situ* formed stabilizers. The sequence of STY in the backbone of the water-soluble copolymer (~14 mol %) should have given a high affinity of copolymer to the interface, and a full coverage of the interface could be reached with a low copolymer concentration. PVA exhibited a moderated influence on the interfacial tension at low concentration, whereas PAA exhibited the lowest influence on the interfacial tension.

Table VII shows the coefficients of the Szyszkowski model estimated by applying eq. (6) to the experimental results of the measures of interfacial tension as a function of the stabilizer concentration. The intensity of absorption (β) showed a great dependence on the kind of suspension agent; the effect of the hydrophobic sequences of STY included in the backbone of the *in situ* formed polymer favored the adsorption of the stabilizer at the interface, as shown in β values. The PAA had the lowest β value because in its structures, there are no hydrophobic sequences attached at the interface.

TABLE VII
Coefficients of the Szyszkowski Model

Suspension agent	Experiment	$\Gamma_S \times 10^{-13}$ (molecules/cm^2)	β (L/g)
AA–STY copolymer	1	5.779	459.94
AA–STY copolymer	6	6.960	1103.60
PVA	9	5.058	26.84
PAA	12	6.540	2.80

Figure 18 shows the surface coverage (θ) estimated by applying the eq. (8); a full coverage of the interface needed a larger amount of the PAA homopolymer than for the *in situ* formed copolymers and also PVA. It has been reported, in the case of absorption experiments of PVA,[24] that several layers are formed around the polystyrene particle to stabilize the polymer particles.

This behavior at the interface could explain the results of the stability system; the protective film formed by PVA was less efficient in preventing the coalescence than the *in situ* formed agent. Although the *in situ* formed agent in experiment 1 gave good control of the PSD in the small sizes, the PVA in experiment 9 allowed the particles to grow, and the final PSD was centered on intermediate values. The same behavior was observed in experiment 2 as compared with experiment 10.

The PAA showed a low affinity to the interface. Its water solutions had the highest values in interfacial tension. The PAA could be adsorbed to the interface; however, it did not form an efficient protective film that prevented the catastrophic coalescence of the system.

Second group of small particles

When the polystyrene beads obtained by our *in situ* process and by the traditional process were filtrated, the remaining water phase was milky, and it became clear only on ultracentrifugation. The solid residue could be redispersed easily in water as a diluted latex, from which the particle size could be measured by quasielastic light scattering. The mean particle sizes of this group of particles was around 100 and 200 nm. Initially, it was thought that the production of these particles was due to a side process of emulsion poly-

merization, which might have come from the use of KPS as initiator in the water phase in the *in situ* process. However, it seemed not to be the case because when the traditional experiments were performed; the remaining water phase was milky, too, but with a lower coloration, due to a smaller amount of particles. Furthermore, in our case, the molecular weight of the polymer from these small particles was about the same as for the polystyrene beads. In addition, NMR analysis indicated that they were composed of pure polystyrene so that a typical emulsion polymerization process could be excluded. Possibly, it may have been related to a strong breakup process and reduction in the interfacial tension.

CONCLUSIONS

It is possible to obtain stable suspensions of polystyrene beads with *in situ* synthesis of the stabilizer (suspension agent) through the polymerization of a water-soluble monomer such as AA. This process allows a good control of the PSD as a function of the ST and the production rate of the *in situ* stabilizer. The water-soluble polymer in our experiment was actually a copolymer of STY and AA containing about 14 mol % STY, even if the solubility of STY in the water phase was low. The copolymer showed high surface-active properties and was located at the interface between the two phases. The high stability of the *in situ* system could be attributed to the high affinity of the STY–AA copolymer to the interface. Then, a good steric stabilizer was strongly adsorbed, providing a thick steric barrier, which was related to its hydrophobic character. The PSD was highly dependent on the conversion of STY, at which the water phase polymerization was started, and it was shifted toward larger sizes if the production of the copolymer was delayed.

The Szyszkowski model described reasonably well the behavior of the suspension agents at the interface and related these observed behaviors with the suspension stability. High values of the β parameter of the model represented a good adsorption of the stabilizer at the interface and might have assured the stability of the suspension system. The stabilizers with STY included in the chains had the highest β values, probably because they were better attached at the interface. The homopolymers of AA, which had the lowest β values, did not correctly prevent the coalescence of the suspension polymerization, whereas copolymers of AA–STY (larger β values) seemed to be well adsorbed into the oil–water interface, resulting in better stabilizers than PVA for the STY suspension polymerizations.

APPENDIX

Kinetics model

Polymerization in each suspension droplet may be considered a microbulk monomer polymerization, and it proceeds through the same kinetic mechanism of bulk polymerization; this assumption is valid for a water-insoluble or a slightly water-soluble monomer, such as styrene.

Copolymerization kinetics parameters

The pseudoconstants for the propagation reaction (kp), chain transfer to the monomer (*ktm*), termination by disproportionation (*ktd*), and termination by combination (*ktc*) are given by the following equations:

$$kp = \sum_{i=1}^{N} kp_{ij}\phi_i^* f_j$$

$$ktm = \sum_{i=1}^{N} ktm_{ij}\phi_i^* f_j$$

$$ktd = \sum_{i=1}^{N}\sum_{j=1}^{N} ktd_{ij}\phi_i^*\phi_j^*$$

$$ktc = \sum_{i=1}^{N}\sum_{j=1}^{N} ktc_{ij}\phi_i^*\phi_j^*$$

where N is the number of monomers, kp_{ij} and ktm_{ij} are the kinetics rate constants for propagation and chain transfer to the monomer, respectively, and the subscripts i and j are used to designate the types of polymer radical and monomer, respectively. The kinetics rate constants ktd_{ij} and ktc_{ij} are for termination reactions by disproportionation and combination, respectively. The molar fraction of radical of type i is ϕ_i^*, namely

$$\phi_i^* = \frac{[R_i^*]}{\sum_{i=1}^{N}[R_i^*]}$$

where $[R_i^*]$ is the radical concentration of the polymer whose radical is located on monomer unit i. The molar fraction of monomer j in the reaction mixture is f_j namely

$$f_i = \frac{[M_j]}{\sum_{j=1}^{N}[M_j]}$$

Based on the application of the method of moments to the mass balance for each of the existing species in the polymerization mix, the live and dead polymer chain-length distribution moments are defined as follows. The *i* moment for live polymer

$$Y_i = \sum_{n=1}^{\infty} n^i[\mathrm{R}_n^*]$$

The *i* moment for dead polymer

$$Q_i = \sum_{n=1}^{\infty} n^i[\mathrm{P}_n]$$

where $[R_n^*]$ and $[P_n]$ represent the concentration of live and dead polymer chains with length n, respectively. The following set or ordinary differential and algebraic equations are obtained with the consideration that $Y_2 \gg Y_1 \gg Y_0$.

Moments of dead polymer concentration distribution are defined as follows. Zeroth

$$\frac{1}{V}\frac{d([Q_0]V)}{dt} = -\frac{1}{2}K_{tc}Y_0^2 + K_{trm}[\mathrm{M}]Y_0$$

First

$$\frac{1}{V}\frac{d([Q_1]V)}{dt} = -K_{tc}Y_0Y_1 + K_{trm}[\mathrm{M}]Y_1$$

Second

$$\frac{1}{V}\frac{d([Q_2]V)}{dt} = -K_{tc}(Y_0Y_2 + Y_1^2) + K_{trm}[\mathrm{M}]Y_2$$

Moments of the live polymer concentration distribution are defined as follows. Zeroth

$$Y_0 = \left(\frac{(2fK_d[\mathrm{I}])}{K_{tc}}\right)^{1/2}$$

First

$$Y_1 = \left(\frac{(2fK_d[\mathrm{I}]) + K_p[\mathrm{M}]Y_0}{K_{tc}Y_0 + K_{trm}[\mathrm{M}]}\right)^{1/2}$$

Second

$$Y_1 = \left(\frac{(2fK_d[\mathrm{I}]) + 2K_p[\mathrm{M}]Y_1}{K_{tc}Y_0 + K_{trm}[\mathrm{M}]}\right)^{1/2}$$

where V is the volume of the reacting mix, f is the initiator efficiency, d/dt represents the rate of change with time, and brackets indicate concentration. M_n and M_w are calculated with moments of the chain length distribution as follows:

$$M_n = MW_M\frac{Q_1 + Y_1}{Q_0 + Y_0}$$

$$M_w = MW_M\frac{Q_2 + Y_2}{Q_1 + Y_1}$$

Diffusion limitations at high conversions lead to a dramatic decrease in the termination rate, resulting in an autoacceleration of the polymerization, a phenomenon known as the Tromsdorff, Norrish–Smith, or gel effect. At even higher conversions, propagation becomes diffusion controlled, and eventually, polymerization stops (the glass effect).

References

1. Winslow, F. H.; Matreyek, W. Ind Eng Chem 1951, 43, 1108.
2. Vivaldo-Lima, E.; Wood, P. E.; Hamielec, A. E. Ind Eng Chem Res 1997, 36, 939.
3. Yuan, H. G.; Kalfas, G.; Ray, W. H. J Macromol Sci Rev Macromol Chem Phys C 1991, 31.
4. Alvarez, J.; Alvarez, J.; Hernández, M. Chem Eng Sci 1993, 48, 1.
5. Chatzi, E. G.; Kipparissides, C. Chem Eng Sci 1994, 49, 5039.
6. Mikos, A. G.; Takoudis, C. G.; Peppas, N. A. J Appl Polym Sci 1986, 31, 2647.
7. Arai, K.; Konno, M.; Matunaga, Y.; Saito, S. J Chem Eng Jpn 1977, 10, 325.
8. Konno, M.; Arai, K.; Saito, J. J Chem Eng Jpn 1982, 15, 131.
9. Villalobos, M. A. Master's Thesis, McMaster University, 1989.
10. Vilchis, L.; Rios, L.; Guyot, A.; Guillot, J.; Villalobos, M. A. 6th International Workshop Polymer Reaction Eng; DECHEMA Monograph; Frankfurt, Germany, 1998; Vol. 134, p 249.
11. Kalfas, G.; Ray, W. H. Ind Eng Chem Res 1993, 32, 1822.
12. Villalobos, M. A.; Hamielec, A. E.; Wood, P. E. J Appl Polym Sci 1993, 50, 327.
13. Wang, S.; Poehlein, G. W. J Appl Polym Sci 1983, 49, 991.
14. Cutié, S. S.; Smith, P. B.; Henton, D. E.; Staples, T. L.; Powell, C. J Polym Sci Part B: Polym Phys 1997, 35, 2029.
15. Gromov, V. F.; Galperina, N. I.; Osmanov, T. O.; Khomikovskii, P. M.; Abkin, A. D. Eur Polym J 1980, 16, 529.
16. Shoaf, G. L.; Poehlein, G. W. Ind Chem Res 1990, 29, 1701.
17. Prausnitz, J. M.; Lichtenthaler, R. N.; De Acevedo, E. G. Molecular Thermo-Dynamics and Fluid-Phase Equilibria, 2nd ed.; Prentice Hall: Upper Saddle River, NJ, 1986.
18. Wang, Z. L.; Pla, F.; Corriou, J. P. Chem Eng Sci 1995, 50, 2081.
19. Mendizabal, E.; Castellanos-Ortega, J. R.; Puig, J. E. Colloids Surf 1992, 63, 209.
20. Olayo, R.; García, E.; Garcia-Gorichi, B.; Sánchez-Vázquez, L.; Alvarez, J. J Appl Polym Sci 1998, 67, 71.
21. Janssen, J. J. M.; Boon, A.; Agterof, W. G. M. Colloids Surf 1994, 91, 141.
22. Oldshue, J. Y. Fluid Mixing Technology; Chemical Engineering Series; McGraw-Hill: New York, 1983.
23. Vincent, B. Adv Colloid Interface Sci 1974, 4, 193.
24. Dequatre, C.; Duhamel, T.; Hermant, A.; Pla, F. Macromol Symp 1995, 92, 301.